ELSEVIER

Polymer 44 (2003) 2041–2047

polymer

www.elsevier.com/locate/polymer

Percolation cluster on partially dissolving polymer film

Şaziye Uğur, Önder Pekcan*

Department of Physics, Istanbul Technical University, 80626 Maslak Istanbul, Turkey

Received 30 July 2002; received in revised form 28 November 2002; accepted 20 January 2003

Abstract

Steady state fluorescence (SSF) technique was used for studying dissolution of UV-induced polymer films. These films are formed from poly(methyl methacrylate) (PMMA) chains labeled with pyrene (P) which was introduced as a fluorescence probe to monitor the dissolution processes. PMMA films in various ethylene glycol dimethacrylate (EGDM) content, cured by UV radiation, were dissolved in chlorofrom–heptane (20–80%) mixtures. Dissolution of the films were monitored in real-time by the P fluorescence intensity change in the solvent reservoir. It is observed that P intensity decreased dramatically above a critical EGDM content, which was atributed to the formation of a percolation cluster. The measured percolation threshold, ($p_c = 0.25$) was found to be in accord with the bond percolation model. Desorption coefficients, D_d were measured for films prepared with various EGDM content and it was observed that D_d values are much lower above p_c than below p_c.

Keywords: Fluorescence; Dissolution; Percolation

1. Introduction

Many of the physical properties of a polymer can be profoundly modified by changes in molecular weight due to crosslinking which at first results in a slight increase in molecular weight, and then by the formation of a network, which can result in a complete change in mechanical behaviour. Polymer network formation can be produced by chemical means, or by radiation [1–3] which has great advantages for quantitative analysis and study of resultant physical behaviour. The physical behaviour and especially the mechanical properties of long chain polymers depend not only on chemical structure and applied temperature, but also on the connectivity between adjacent molecules. Many of physical properties dependent on crosslink density are also influenced by chain entanglements, which can behave for limited periods as equivalent to prominent crosslinks.

Crosslinking can be produced in long chain polymers by a number of chemical reagents, but also by high energy radiation. Characteristic for the radiation-induced crosslinking can be initiated at low temperatures by simply placing polymer specimen into the radiation field. Moreover crosslinking occur spontaneously without the aid of added low molar mass additives. Radiation is a convenient tool to alter physical properties of polymers, since crosslinking cause alterations in the average molar mass and many practically important physical properties depend on the molar mass [3].

The simplest form of crosslinking is one where two radicals on adjacent molecules are linked together to form a direct crosslinking [4]. The first chance is merely an increase in molecular weight as when two linear molecules are linked at random, which present a small increase in viscosity, although the weight average M_w, will show a greater change. The above process is called as gelation which is the phase transition from a state without a gel to a state with a gel i.e. gelation involves the formation of an infinite network. In the sol–gel phase transition, an infinitely large macromolecule is formed which is called a gel. The conversion factor p is the fraction of bonds which have been formed between the monomers of the systems, i.e. the ratio of the actual number of bonds at the given moment to the maximally possible number of such bonds [5,6]. Thus for $p = 0$ no bonds have been formed and all monomers remain isolated. In the other extreme, $p = 1$, all possible bonds between monomers have been formed and thus all monomers in the system have clustered into one

* Corresponding author. Tel.: +90-212-285-32-13-32-62; fax: +90-212-285-63-86.
E-mail address: pekcan@itu.edu.tr (O. Pekcan).

0032-3861/03/$ - see front matter © 2003 Elsevier Science Ltd. All rights reserved.
PII: S0032-3861(03)00074-0

infinite network, with no sol phase left. Thus for small p no gel is present whereas for p close to unity one such network exists. Therefore, there is in general a sharp phase transition at some intermediate critical point $p = p_c$, where an infinite cluster starts to appear; a gel for p above p_c, a sol for p below p_c. This point $p = p_c$ is the gel point and may be the analog of liquid–gas critical point [5].

Polymethyl methacrylate (PMMA) film dissolution was first studied using laser interferometry by varying molecular weight and solvent quality [7]. Winnik and co-workers modified the interferometric technique and studied the dissolution of fluorescence labeled PMMA films [8] by monitoring the intensity of fluorescence from the film together with the interferometric signal. The solvent penetration rate into the film and the film dissolution were measured simultaneously. Fluorescence quenching and depolarization methods have been used for penetration and dissolution studies in solid polymers [9–11]. The real-time, non-destructive method for monitoring small molecule diffusion in polymer films has been developed [12–15]. This method is based on the detection of excited fluorescence dyes desorbing from a polymer film into a solution in which the film has been placed. A steady state fluorescence (SSF) study on dissolution of both annealed latex film [16] and PMMA discs using real-time monitoring of fluorescence probes [17] were reported. Recently effect of γ-irradiation on latex film dissolution was studied using SSF [18]. Fast Transient fluorescence (FTRF) technique was recently applied to investigate polymer dissolution [19].

The mechanism of polymer film dissolution is much more complicated than small molecule dissolution. Small molecule dissolution can be explained by Fick's law of diffusion with a unique diffusion rate [20]. However, in polymeric systems many anomalies or deviations from Fick's law of diffusion are observed [21], particularly below the glass transition temperature of a polymer. In general this question of non-Fickian or anomalous diffusion can be perhaps subdivided into two sub-sections. The first concerns sorption of solvent into the glassy polymers. The second deals with the relaxation of polymer chains in the swollen gel layer. The most characteristic feature of the former is that the amount of solvent sorbed into the polymer varies with time raised to an exponent between 0.5 and 1.0, where the extreme case (1.0) is called Case II diffusion. After the completion of the swollen gel layer, polymer chains start to desorb according to case I diffusion which is also called Fickian diffusion. The final step of polymer dissolution is called mutual diffusion of the polymer and solvent molecules in liquid phase.

In this work dissolution of PMMA films induced by UV radiation was studied in chloroform–heptane mixture using SSF technique. Good-bad solvent mixture was preferred to initiate and control the partial dissolution processes. Controlled dissolution process reduces the errors on fluorescence intensity. Various films in various crosslinker ethylene glycol dimethacrylate (EGDM) content were prepared and irradiated with UV light to form a network before dissolution. In situ SSF experiments were performed to observe the partial dissolution processes. Partial dissolution experiments were designed so that PMMA labeled P molecules, desorbing from films, were detected in real-time monitoring of SSF intensity. Desorption rate, D_d were measured using curves of intensity versus time. Maximum P intensity, I_{pm} was measured after dissolution process is completed for each film sample at various EGDM content. It was observed that I_{pm} decreased dramatically above a critical value of EGDM. The decrease in I_{pm} was explained with the formation of a percolation cluster at this critical value in the UV-induced film. D_d values are found to be much lower above the percolation threshold, p_c, than below p_c.

2. Theoretical considerations

2.1. Percolation model

Initially the percolation theory has been associated with a paper of Broadbent and Hammersley which discussed the general situation of a fluid spreading randomly through a medium [22]. The most interesting feature of percolation phenomenon is the existence of a percolation threshold, p_c below which spreading process is confined to be a finite region. The spread of a blight from tree to tree in an orchard was discussed by Broadbent and Hammersley where the trees are planted on intersection of a square lattice. The percolation threshold, p_c for this problem is around 0.6 for so called 'site percolation' on a square lattice. In other example is the seepage of water in the cracks and fractures of a rock formation. A similar problem for practical interest is the spread of water displacing oil in porous rocks, where neighbouring pores are connected by small capillary channels [23]. If no oil in the system injected water into any given pore may only invade another pore through capillary channels or 'bonds'. The pores are 'sites' connected to the chosen centre of injection form what is called a 'cluster'. The largest cluster spans the lattice connecting the left and right edges to the bottom edge, which is called 'percolating cluster'. The percolation probability, $p_\infty(p)$, is defined as the probability that water injected at a site, chosen at random, will wet infinitely many pores. Here one has to be noticed that the probability for having a pore at all the sites where water injection is attempted is p. Extensive simulations and theoretical work have shown that the percolation probability vanishes as a power-law near p_c:

$$p_\infty(p) \approx (p - p_c)^\beta \tag{1}$$

for $p > p_c$, and $p \to p_c$. In a simple cubic lattice p_c is found to be 0.31 for site-percolation and 0.249 for bond

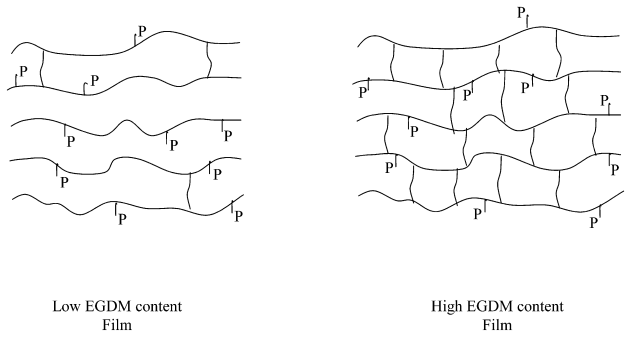

Fig. 1. Cartoon representation of the films prepared at high and low EGDM content.

percolation models [5]. The exponent β for a simple cubic lattice is 0.45.

2.2. Fickian desorption

The classical diffusion model was applied to interpret the results of polymer dissolution experiments. This model includes only case I diffusion kinetics, because no gel layer was observed during the dissolution at early times, most probably gel layer was eliminated using continuous agitation. Case I or Fickian diffusion model includes the solution of a unidirectional diffusion equation for a set of boundary conditions which is sited by Crank [20]. For a constant diffusion coefficient, D and fixed boundary conditions, the absorption and dissolution transport in and out of a thin slab is given by the following relation

$$\frac{M_t}{M_\infty} = 1 - \frac{8}{\pi^2}\sum_{n=0}^{\infty}\frac{1}{(2n+1)^2}\exp\left(\frac{-(2n+1)^2 D\pi^2 t}{d^2}\right) \quad (2)$$

Here, M_t represents the amount of materials absorbed or desorbed from the thin slab at time t, M_∞ is the equilibrium amount of material, and d is the thickness of the slab. n comes from the solution of diffusion equation in the form of a trigonometrical series.

3. Experimental

3.1. Material

In this work, initially polymeric latex particles were used in UV-induced film formation. The poly(isobutylene) (PIB) sterically stabilized PMMA latexes were prepared separately in a two-step process [24,25]. In the first step, short PMMA squences were grafted onto PIB sample of nominal molecular weight 10^4. These PIB samples contain sites of unsaturation for reaction with either initiator radicals or growing PMMA chains. Polymerization is terminated before the PMMA sequences become sufficiently long as to render the polymer insoluble in the cyclohexane reaction mixture. This short graft copolymer, called the 'dispersant' is precipitated from solution with ethanol and purified. In the second step of preparation, the dispersant methyl methacrylate (MMA), an initiator, 1-pyrenyl methyl methacrylate (P-MMA) are combined in cyclohexane solution and refluxed over night. A white dispersion forms. This procedure produces spherical particles of relatively narrow distribution of sizes. Using P-PMMA as the comonomer yielded latexes containing P groups covalently bound to the PMMA. These material was freeze-dried from cyclohexane, stored as a powder. The compositions of material were determined by NMR and UV absorption studies of their solutions in $CDCl_3$ and ethyl acetate respectively. These analysis indicated that these particles contain 4 mol %PIB and 0.037 mmol P groups per gram of polymer.

3.2. Film preparation

The film preparation were carried out in the following manner; these P labeled PMMA particles were dissolved in chloroform and 5% photoinitiator (irgacure) was added in the solution. Then using this stock solution twelve different films were prepared by adding different amount of EGDM (0, 6, 17, 25, 35, 42, 46, 51, 56, 59, 65 and 70 wt%) in to the twelve different test tubes. Twelve different films prepared by placing these solutions onto the $0.8 \times 2.5\ cm^2$ glass plates and let them to dry in air. These films were then induced by UV radiation for 25 hours in a merry go round type photoreactor equipped with 15 Philips Lamps, which emitting light nominally at 350 nm at room temperature. Here basically irgacure absorbs light from photoreactor and forms the radicals. These radicals extracts hydrogen from the precursor PMMA polymer. The formed polymeric radicals then initiate the polymerization reaction in EGDM due to the bifunctional nature of this monomer. Finally, at the end of the polymerization reaction insoluble, crosslinked network is formed. The thicknesses of the prepared films were measured and found to be around 30 μm. Films were weighted before and after dissolution to measure the amount of dissolved PMMA material. Cartoon representation of the networks in the prepared films at low and high content EGDM are presented in Fig. 1.

3.3. Fluorescence measurements

In situ fluorescence experiments were performed using a Perkin Elmer LS-50 spectrofluorimeter. All measurements were made at 90° position and the slit widths were kept at 10 nm. Dissolution experiments were performed in a $1 \times 1\ cm^2$ quartz cell which was placed in the spectrofluorimeter. The fluorescence emission was monitored so that film samples were not illuminated by the excitation light. Samples were placed at one side of a quartz cell filled with chloroform–heptane mixture (80–20%) and cell was then illuminated with 345 nm excitation light. The pyrene fluorescence intensity, I_P, was monitored during the partial dissolution process at 395 nm using the 'time drive' mode of

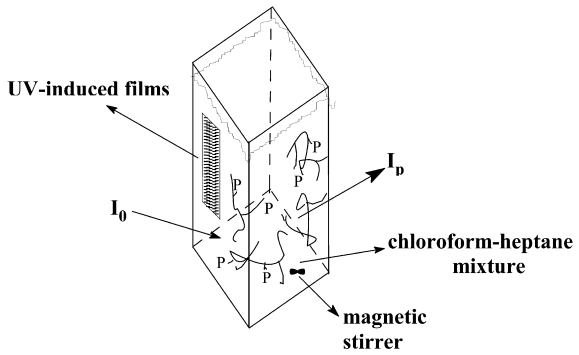

Fig. 2. Fluorescence cell as used in LS-50 Perkin Elmer Spectrofluorimeter. I_0 and I_P are the excitation and emission intensities at 345 and 395 nm, respectively.

the spectrofluorimeter. Emission of P was recorded continuously at 395 nm as a function of time. No variation in P spectra was observed before and after the irradiation and during dissolution processes. The cell and the sample position are presented in Fig. 2. Here the 1×1 cm^2 quartz cell was equipped with a magnetic stirrer at the bottom. During the fluorescence measurement no light scattering was observed at the excitation wavelength.

4. Results and discussion

Plots of P intensity, I_P versus partial dissolution time, t for the films prepared with various EGDM content and induced by UV radiation at low stirring speed are shown in Fig. 3. Numbers on each curve present the EGDM content (wt%). It is seen that, all curves increase at early times by reaching a plateau at later times, presenting an exponential behaviour. It has to be noted that low EGDM content samples (including zero EGDM sample) present higher dissolution rate than high EGDM content samples which may effect the calculation of D_d values. On the other hand at time $t = 0$ some intensity curves do not start from zero. This error originates mostly from the start up time of the time drive mode of the spectrofluorimeter. Namely, time is turned on after film is placed into the fluorescence cell filled with solvent. Another error comes from the signal to noise ratio. I_P curves reached the plateau at different values depending on the EGDM content used in the film. The maximum emission spectra of P at infinity time I_{pm} (i.e. at the plateau) are plotted versus EGDM content in Fig. 4a. It is seen both in Figs. 3 and 4a that maximum P intensities, I_{pm} are much lower for high EGDM content film samples than low EGDM film samples. In fact I_{pm} values drop dramatically above the critical, 25 wt% EGDM content samples, i.e. film samples contain more than 25 wt% of EGDM dissolve much less. However film samples with low EGDM content dissolve much easier, indicating that some of the PMMA chains are slightly crosslinked and form small clusters in the film. Above the critical EGDM content

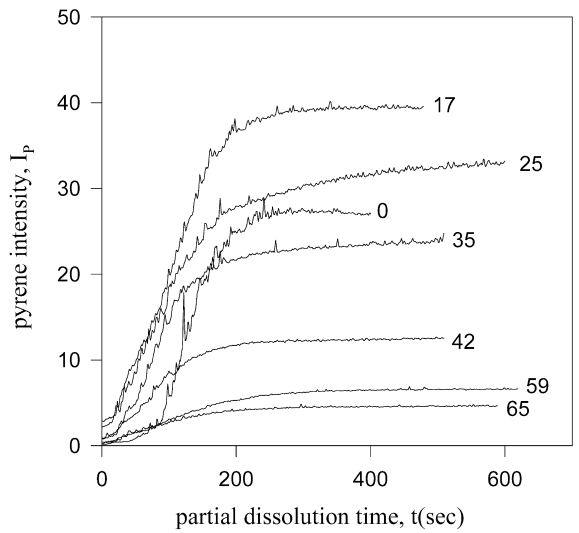

Fig. 3. Pyrene intensity, I_P, versus partial dissolution time for the UV cured film samples dissolved in chloroform–heptane mixtures at low stirring speed. Numbers on each curve present the amount of EGDM in wt%.

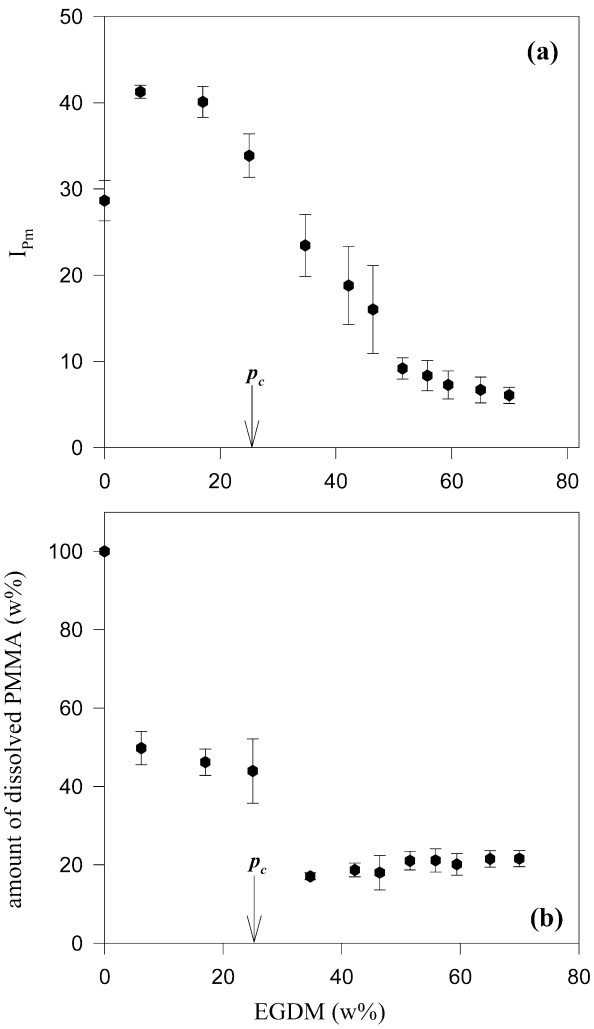

Fig. 4. The plots of (a) the maximum pyrene intensity, I_{pm} (b) the amount of dissolved PMMA material versus EGDM content for UV-induced films.

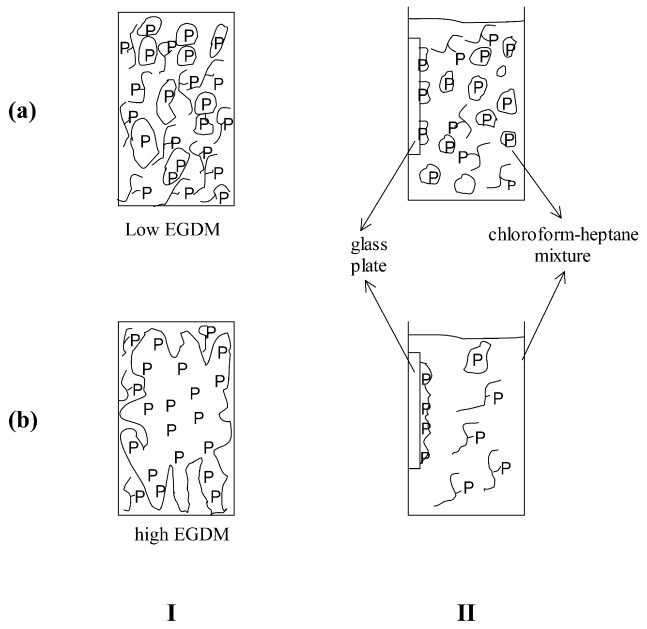

Fig. 5. Cartoon represantation of I- UV-induced films at (a) low, (b) high EGDM contents. Dissolution of these films are shown in IIa and IIb respectively.

(25 wt%) low I_{pm} values indicate that most of the PMMA chains are highly crosslinked by forming large clusters which prevent the film from dissolution. In fact films with very high (more than 50 wt%) EGDM content form infinite clusters which are very difficult to dissolve. Most probably percolation cluster is formed in 25 wt% EGDM ($p_c = 0.25$) content film.

UV-induced film samples were weighted before and after partial dissolution experiments are completed, from which amount of dissolved PMMA are measured and are presented in Fig. 4b. It is seen that below the critical point (25 wt% of EGDM), 45% of PMMA dissolve from the UV induced samples. On the other hand 20% of PMMA dissolved when the film samples prepared by adding more than 25 wt% EGDM and induced by UV radiation. These findings predict that above 25 wt% EGDM inclusion, creates large PMMA clusters in film samples which are difficult to be dissolved. Cartoon representations of this picture are given in Fig. 5 where film with low EGDM and induced by UV radiation contain small clusters or free PMMA chains (Ia) and dissolved partially (IIa). Film formed with high EGDM and induced by UV contains large cluster (Ib) and hardly dissolve (IIb). Here one has to be noticed that the critical EGDM value, 25 wt% most probably corresponds to the p_c for the bond percolation at which the largest cluster spans the lattice by connecting the left and right edges to the bottom edge [5] (see Fig. 4–Ib). The behaviour of I_{pm} and amount of dissolved PMMA in Fig. 4a and b confirm the formation of the percolation cluster at ($p_c = 0.25$). If one assumes that the bond formation probability, p is equal to the wt% EGDM content in the film sample then data in Fig. 4a can be treated according to Eq. (1). The percolation probability now becomes the gel fraction [5,6] where pyrenes are embedded. Since I_{pm} is proportional to the amount of dissolved polymeric material $(1 - I_{pm}/I_{Pm0})$ gives information about the undissolved part of the polymeric material i.e. $(1 - I_{pm}/I_{Pm0})$ is proportional to the gel fraction formed on the partially dissolved film. Here I_{Pm0} is the I_{pm} from the lowest EGDM content sample. The plot of $(1 - I_{pm}/I_{Pm0})$ versus P is shown in Fig. 6a. The slope of the log–log plot of the curve in Fig. 6a produces critical exponent β as 0.55 which is somewhat larger than the value known for simple cubic ($\beta = 0.45$). Result is shown in Fig. 6b.

The curves in Fig. 3 seem to follow a Case I (Fickian) diffusion model. In processing the dissolution data, it is assumed that I_p is proportional to the number of P labeled PMMA chains dissolving from the UV-induced PMMA film. Here it is assumed that unattachment process follows natural desorbtion by obeying case I diffusion model. It has to be also noted that saturation of I_P curves strongly suggest that unattachment process is completed and desorption of

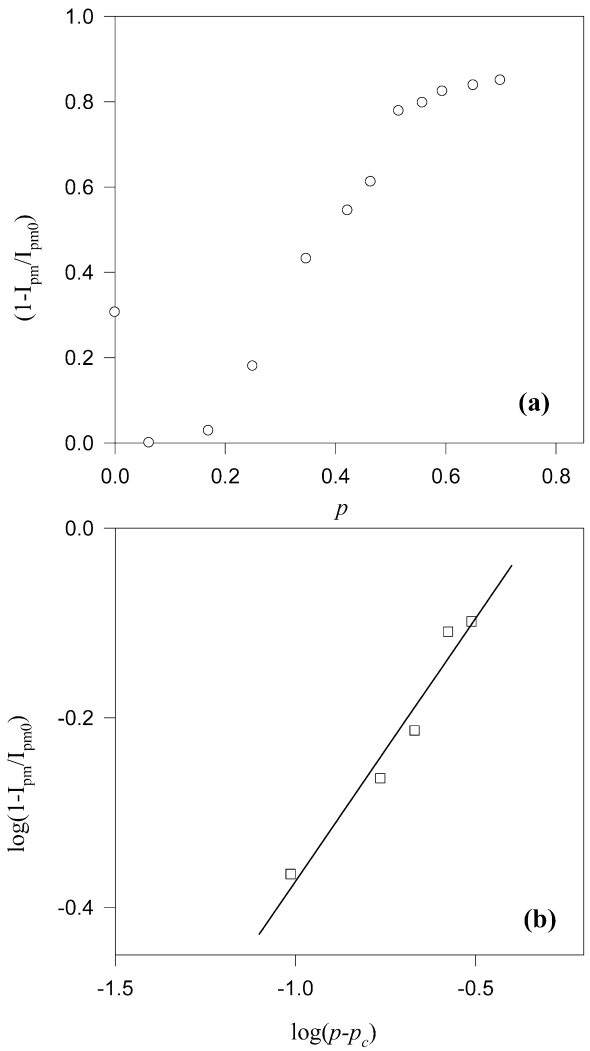

Fig. 6. The plot of the percolation probability versus bond formation probability.

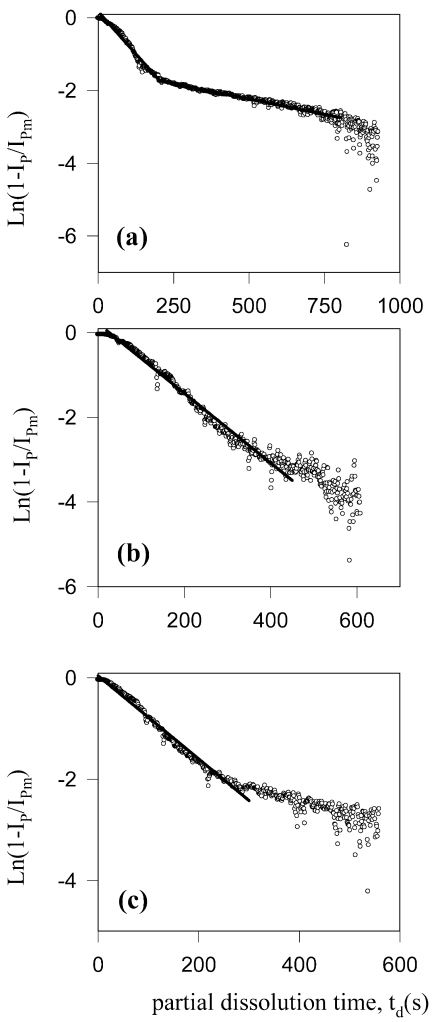

Fig. 7. Partial dissolution curves fitted to Eq. (3) for the film samples formed with (a) 25, (b) 51 and 60 wt% EGDM.

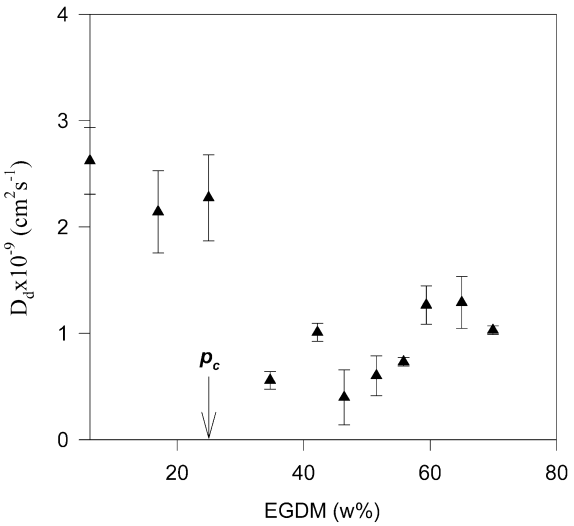

Fig. 8. Plot of desorption coefficient, D_d versus EGDM content.

PMMA chains reached to an equilibrium. The logarithmic form of Eq. (2) is written for $n = 0$, with $A_d = D_d\pi^2/d^2$ and $B_d = \mathrm{Ln}(8/\pi^2)$ as follows

$$\mathrm{Ln}(1 - I_P/I_{pm}) = B_d - A_d t \quad (3)$$

Here, I_{pm} presents the number of P molecules at equilibrium condition, D_d is the desorption coefficient and d is the thickness of the latex film. Fig. 7a–c present partial dissolution curves accord with Eq. (3) for films formed with 25, 51 and 60 wt% EGDM, respectively. It is interesting to state that with 25 wt% EGDM sample present two sequential regimes namely fast and slow, which confirm the picture in Fig. IIa. In others words 25 wt% EGDM film sample desorbs two different weight of PMMA materials; at early times low molecular weight PMMA chains dissolve, however at later times small clusters go into the solvent reservoir. Here slight deviation from linearity at early times in Fig. 7a can be explained with the case II diffusion, which concerns with the formation of a swollen gel layer. In other words the effect of magnetic stirrer is unable to remove the gel layer completely from the surface of the polymer film [16]. In data analysis the influence of case II diffusion at early times of dissolution was neglected and case I diffusion model was employed. On the other hand film samples 51 and 60 wt% EGDM show single dissolution behaviour belong to low molecular weight PMMA chains. Data in Fig. 7 are digitized for numerical treatment. When these linear curves in Fig. 7a–c are compared to computations using Eq. (3), desorption coefficient, D_d for P labeled PMMA materials are obtained, and are plotted in Fig. 8 together with other samples against EGDM content. Results in Fig. 8 support our previous arguments, where low crosslinked films dissolve much faster than high crosslinked films. High crosslinked films above p_c dissolve at least 2.5 times slower than low crosslinked films as pointed out in Fig. 8.

In summary this work presented the results obtained from the partial dissolution of UV-induced polymeric films. The film formed a percolating cluster during partial dissolution if it contains 25 wt% crosslinker and exposed to UV radiation for 25 h. These films dissolved much faster below p_c and partially dissolved above p_c, producing high and low desorption coefficients, D_d.

Acknowledgements

We would like to thank Prof. Y. Yağci for his fruitful and stimulating ideas.

References

[1] Makhlis A. Radiation of physics and chemistry of polymers. New York: Wiley; 1975.
[2] Kloosterboer JG. Adv Polym Sci 1988;84:1.
[3] Vollenbroek FA. Adv Polym Sci 1988;84:85.

[4] Florry PJ. Principles of polymer chemistry. Cornell; 1953.
[5] Stauffer D. Introduction to percolation theory. London: Taylor and Francis; 1985.
[6] Stauffer D. Pure Appl Chem 1981;53:1479.
[7] Krasicky PD, Groele RJ, Rodriquez F. J Appl Sci 1988;35:641.
[8] Limm W, Dimnik GD, Stanton D, Winnik MA, Smith B. J Appl Polym Sci 1988;35:2099.
[9] Guilet JE. In: Winnik MA, editor. Phototphysical and photochmical tools in polymer science. Dordrecth: Reidel; 1986.
[10] Nivaggioli T, Wank F, Winnik MA. J Phys Chem 1992;96:7462.
[11] Pascal D, Duhamel J, Wank J, Winnik MA, Napper Dh, Gilbert R. Polymer 1993;34:1134.
[12] Lu L, Weiss RG. Macromolecules 1994;27(1):219.
[13] Kronganz VV, Mooney III WF, Palmer JW, Patricia JJ. J Appl Polym Sci 1995;56(9):1077.
[14] Kronganz VV, Yohannan RM. Polymer 1990;31(9):1130.
[15] He Z, Hammond GS, Weiss RG. Macromolecules 1992;25(1):501.
[16] Pekcan Ö, Uğur Ş, Yilmaz Y. Polymer 1997;38:2183.
[17] Uğur Ş, Pekcan Ö. Polymer 1997;38:5579.
[18] Aydın K, Uğur Ş, Pekcan Ö. J Coll Inter Sci 2001;233:91.
[19] Uğur Ş, Pekcan Ö. Polymer 2000;41:1571–5.
[20] Crank J. The mathematics of diffusion. Oxford: Clarendon Press; 1975.
[21] Crank J, Park GS. Diffusion in polymer. London: Academic Press; 1968.
[22] Broadbent SR, Hammersley JM. Proc Camb Phil Soc 1957;53:629. Frisch HL, Hammersley JM. J Soc Industr Math 1963;11:894.
[23] Sahimi M. Applications of percolation theory. London: Taylor and Francis; 1994.
[24] Barrett KEJ, editor. Dispersion polymerisation in organic media. London: Wiley-Interscience; 1975.
[25] Pekcan Ö, Winnik MA, Egan L, Croucher MD. Macromolecules 1983;16:699.